# A 34 element 3T Brain coil array for multi dimensional accelerated imaging

S. A. Lindsay[1], K. F. King[1], J. E. Lorbiecki[1], E. B. Boskamp[1]

[1]Global Applied Science Lab, GE Healthcare, Waukesha, Wisconsin, United States

## INTRODUCTION

Parallel imaging strategies (1,2) are becoming the principal tool for accelerated clinical MR imaging. The competing constraints between (i) available baseline signal-noise-ratio (SNR), (ii) noise amplification (g-factor) and (iii) achievable acceleration factor (R) represent a fundamental challenge for clinical parallel imaging applications. The use of multi-dimensional coil arrays consisting of large numbers of elements can improve SNR and hold the promise to reduce noise amplification which requires tailored coil configurations for different applications. This study is aiming at the design of a 3T proton 34 channel brain coil customized for multidimensional parallel imaging brain applications using multi-oblique imaging planes. The coil arrays performance was examined (i) in phantom studies and (ii) in volunteer studies using high spatial resolution anatomical $T_1$ weighted imaging together with multi-dimensional net acceleration factors of up to 9 (R=3x3). The 34 channel was chosen as the preferred configuration at 3T, where patient loading keeps the diameter, at which coil elements become coil noise dominated, down to about 4-5 cm (3). Going to even more channels will not be beneficial for baseline SNR.

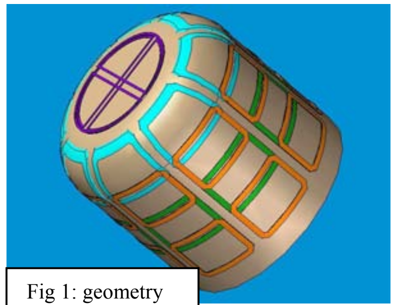
Fig 1: geometry

## MATERIAL AND METHODS

The coil was built onto a fiberglass epoxy former, in the shape of a dome (fig 1). The axial cross section is elliptical with long and short axes of 255 and 220 mm. The length of the coil in the z direction is 180 mm to cover from apex to brain stem. On the cylindrical portion of the coil 3 layers of 8 elements are applied. The elements are rectangular with dimensions of 80 mm in the tangential direction and 55 mm in the z direction. Neighboring layers are overlapped in the z direction by about 10 mm to prevent direct neighbor coupling and signal drop out in sagittal and coronal images. In the tangential direction the elements are separated by about 10 mm to provide for better g factor. Decoupling between direct neighbors is achieved via transformers. In the spherical section of the coil a 4th layer of 8 trapezoidal elements is added. Dimensions are 80 and 50 mm for the base and top, and 55 mm for the height. To complete the coil, 2 perpendicular elliptical butterfly elements are added to the apex. A PIN diode switch allows activation of any subset of 32 coils out of the 34 channel array as needed on a 32 receive channel system. Dimensions of the long and short axes are 100 and 90 mm. A drawing of the coil configuration is shown in fig 1. As indicated, better than 20 dB isolation is achieved between direct neighbors either via overlap or transformer decoupling. Other possible coupling is prevented by using low input impedance (1.5 ohms) directly on the coil elements, as shown in the picture in fig 2. The decoupling impedance achieved by the preamp placement is in the order of 150 ohms. Spherical phantom (diameter 180 mm, concentration: $1.4x10^{-2}$ molar Nickel Chloride) images were used to measure the geometry factor maps for different planes and acceleration factors and to compare them to the simulated values. A 2D spin echo sequence (TE/TR = 20/1000, +/-32 kHz receive bandwidth, 10 mm slice, 256x128, 1 average) was used for the phantom images. Volunteer images were made with a 3D $T_1$ weighted, IR-prepared, gradient echo sequence (TE/TI/TR = 3/450/6.2, flip = 12, +/-32 kHz receive bandwidth, 24 cm field of view, 1.5 mm slice, 256 x 256, 3:36 unaccelerated). Acceleration factors up to three in each direction were tested.

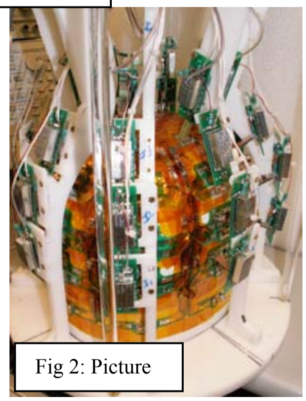
Fig 2: Picture

## RESULTS

Geometry factor images for axial (phase encoding L/R), sagittal (phase encoding A/P) and coronal (phase encoding L/R) planes are shown from left to right for an acceleration factor of 4 (Fig 3) and an acceleration factor of 6 in Fig 4. The mean and maximum of the geometry factor calculated within the phantom is listed in the accompanying table. Fig 5 shows a baseline brain image without acceleration. Figure 6 shows three-fold acceleration in phase and slice (nine-fold total acceleration) including 40 phase and 40 slice Nyquist-sampled self-calibration lines. Generalized SENSE (4) was used to reconstruct the images. Slice width in both was **only 1.5 mm, 256 squared, 1 NEX.**

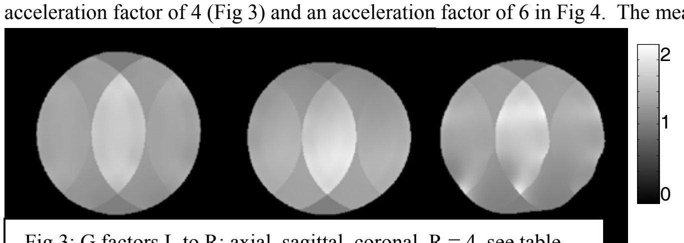

Fig 3: G factors L to R: axial, sagittal, coronal, R = 4, see table

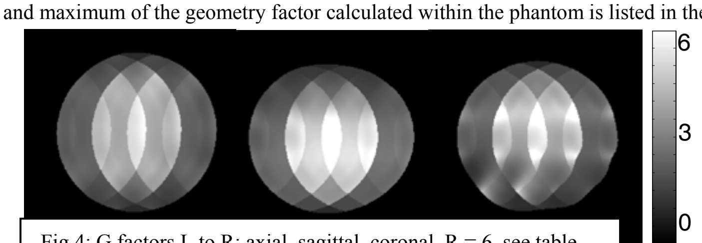

Fig 4: G factors L to R: axial, sagittal, coronal, R = 6, see table

| R | 4 | 4 | 6 | 6 |
|---|---|---|---|---|
| G factor | mean | max | mean | max |
| Axial Phase L/R | 1.3 | 1.7 | 3 | 6 |
| Sagittal phase A/P | 1.3 | 1.9 | 3.3 | 7.6 |
| Coronal phase L/R | 1.3 | 1.9 | 3 | 7.9 |

## DISCUSSION AND CONCLUSION

A 34-element 3T volume brain coil was developed that affords simultaneous accelerations not only along all three main directions but for multi-oblique imaging planes. Noise amplification maps revealed g factors close to one for all 3 cardinal imaging planes up to R = 4. Accelerated images with a total acceleration factor of up to 9 demonstrated the SNR advantage of two-dimensional accelerations using a dedicated coil array design. Such image quality cannot be obtained with similar one-dimensional net acceleration using a circular array consisting of 34 elements distributed circumferentially since the use of many-element RF coil arrays can alleviate noise amplification to some extent, but electro-dynamic constraints dictate that a fairly rapid degeneration of SNR at high one-dimensional accelerations is inevitable (5). In conclusion, further SNR improvements may be expected with the application of three-dimensional accelerations, which are clearly facilitated by the coil design presented here, using non-cartesian k-space trajectories. Consequently, future studies including clinical comparisons are planned with our 34-element brain array.

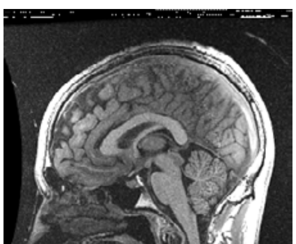
Fig 5: Unaccelerated image

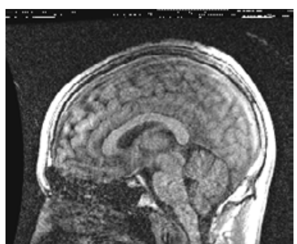
Fig 6: Accelerated image

## REFERENCES

(1) Pruessmann KP et al. Magn Reson Med. 1999; 42:952-962; (2) Weiger M et al. Magma 2002; 14:10-19. ; (3) Boskamp E. et al. Proc ISMRM 13, 2005, p 916 ; (4) Pruessmann KP et al. Magn Res Med 2001; 46:638-651; (5) Ohliger MA et al. Magn Res Med 50, 2003, p1018.